Aalborg Universitet

User Impact on Phased and Switch Diversity Arrays in 5G Mobile Terminals

Syrytsin, Igor A.; Zhang, Shuai; Pedersen, Gert F.

User Impact on Phased and Switch Diversity Arrays in 5G Mobile Terminals

Igor Syrytsin, Shuai Zhang, Gert Frølund Pedersen

Abstract—In this paper, a mobile terminal phased array at 28 GHz with different scan angles is compared to a switch diversity antenna array at 28 GHz in the case of antenna beams pointing at the user's body. In the switch diversity antenna array, there is only one element out of eight operating each time. The study is carried out in data mode with a standing user, which includes both body blockage and user hand effects. The metrics of coverage efficiency, antenna shadowing power ratio and isotropic antenna shadowing power ratio are utilized in the investigation. It is found that the scan angle of a phased array higher than 90° is not necessary for this scenario because the user body will contribute to the total radiation at large angles by scattering the radiated energy around the body. For the linear phased antenna arrays on the edge of the mobile device ground plane it can be concluded that in order to achieve the highest coverage efficiency and lowest user shadowing it is more beneficial to use a phased array instead of a switch diversity array. However, if the losses of the phase shifters and the feeding network from the phased array are higher than 5 dB, the switch array can be used, which will also decrease the complexity of a system.

Index Terms—Mobile Terminal Antenna, 5G antenna, user effects, human shadowing, SAPR, SIAPR, coverage efficiency.

I. Introduction

BECAUSE of the recent technological development in the direction of the fifth generation communication system phased mobile antenna arrays have become a very active research topic. The 5G mm-wave mobile communication system will probably occupy bands in the range from 20 GHz to 40 GHz [1]. At the mm-wave frequencies, the path loss is much higher than at the GSM or LTE frequencies used today. As enabler technology for the 5G in [2], phased mobile arrays can achieve gains up to 10 dBi, and thus can counteract the high path loss at cm or mm-wave frequencies [3], [4]. However, to achieve the best spatial coverage performance, the phased array should be scanned. In order to do that, multiple phase shifters and feeding network are required. Phase shifters with large phase shifts are usually lossy, and thus, will decrease the overall performance of the system when large array scan angles are desired. If a switched diversity (SD) array or a phased array with small phase shift can be applied, the loss of phase shifters can be minimized.

The cellular mobile device can have an arbitrary location when used. The conventional LTE and GSM antennas have an omni-directional radiation pattern but in 5G mm-wave systems the directional antennas with beam agility will be used. Thus, the metric for describing the spatial coverage of the 5G antenna system is needed. The concept of coverage efficiency was introduced in [5]. Then, it has been applied in [6] to characterize 5G mm-wave antennas in mobile terminals and quantify the spatial performance. Furthermore, this metric also takes into account the randomness of the mobile terminal orientation when used by a human. Not only the high spatial coverage of the 5G phased antenna array is important but also the user effects on the performance of phased antenna arrays are a significant issue. Recently it has been found in [7] that human shadowing has a significant impact on the performance of the mobile phased arrays at cm/mm-wave frequencies. Not to mention, even at the GSM/LTE frequencies, a shadowing up to −20 dB from the user's head has been observed in [8]. Most interestingly, the body loss of the mobile antennas at the 28 GHz is insignificant in comparison to the power lost in the shadowing region as described in [9]. Contradictory to the GSM/LTE frequencies, not only the user's head but also a full user's body should be considered for the performance verification of a mobile terminal antenna at the cm/mm-wave frequencies. The performance of the phased antenna array will indeed be affected by the user. A small amount of 1 to 4 dB of absorption loss will be induced [9]. Yet, those numbers are very low in comparison to the GSM frequencies, where absorption loss of 10 to 15 dB has been measured. Furthermore, at the user's effect on the detuning of operating frequency of the cm/mm-wave antenna is not significant. However, the shadowing at the cm/mm-wave frequencies is more severe than at the GSM/LTE frequencies. Thus, coverage efficiency metric cannot be used alone to verify the performance of the mobile terminal with the user. In order to quantify the shadowing effect at 28 GHz in [9] it has been proposed to characterize the shadowing region by means of Shadowing Antenna Power Ratio (SAPR) and Shadowing Isotropic Antenna Power Ratio (SIAPR). Multiple investigations of the human shadowing have been already done for 60 GHz WLAN, but effects of the human hand and arm have not been considered. In [10] a statistical model for human body shadowing has been proposed, but the model does not include the human hand. And finally, in [11] shadowing dependence on the transmission distance and human position between antennas has been investigated at the frequencies up to 30 GHz. However, the user was positioned between the antennas, and not interacting with the mobile device directly. All things considered, a comparison between a phased mobile antenna array and an SD antenna array has not been studied in user case yet.

In this paper, a mobile phased array's and SD array's performance with the user in data mode will be investigated at 28 GHz by applying metrics of SAPR, SIAPR and coverage

This article has been accepted for publication in a future issue of this journal, but has not been fully edited. Content may change prior to final publication. Citation information: DOI 10.1109/ACCESS.2017.2779792, IEEE Access

2

efficiency. In this investigation, it has been chosen to look at the most challenging scenario from the spatial coverage perspective. In this scenario, the base station is located behind the user and the mobile phased array is pointing towards the user's body as shown in Fig. 1. In this scenario, the big shadowing area will be created by the user's body. Thus, it is very interesting to investigate if the phased/SD array can be used in order to reduce that shadowing area. The investigation is carried out by simulating monopole mobile phased array with wide scan angle in CST Microwave Studio FDTD solver. In simulations, a full-body phantom holding a mobile terminal in the left hand has been used. Furthermore, the switch diversity characteristics of the same array are investigated by simulations and measurements with the phantom/user.
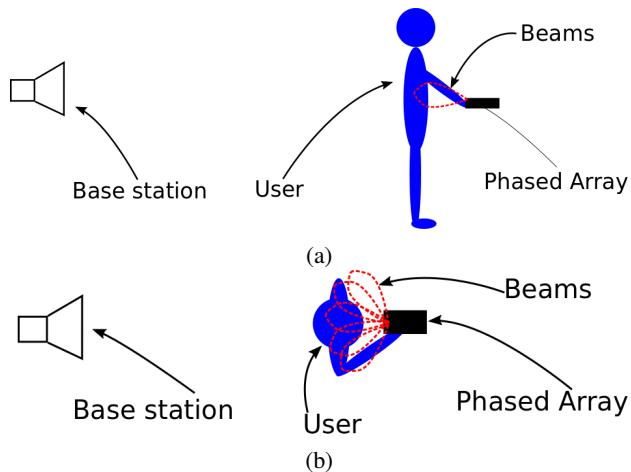

Fig. 1. The scenario where a base station is behind the user and mobile phased array pointing towards the user's body (a) side view and (b) top view.

II. ARRAY FREE SPACE PERFORMANCE

In this paper, the same antenna array has been applied in two manners:

- As a phased array, where different weights are applied on each of the array element and then signals from all elements are summed together. In this study, only the phase has been applied as a weight (imitating real phase shifters in the application).
- As a switch diversity array, where only one antenna is used at a time. In the application, the 1P8T switch could be used for this purpose. One could expect diversity to be implemented through the usage of spatially separated antennas.

For the purpose of this investigation, it has been chosen to construct a simple monopole antenna array which is shown in Fig. 2. One piece of copper of 5 mm height has been added to the design in order to obtain the desired endfire radiation pattern, and suppress the surface wave. Because in the investigation, the wide scan angle of the phased antenna array is needed, the monopole array elements have been applied. The monopole array elements have an omnidirectional radiation pattern characteristics, which makes the perfect for
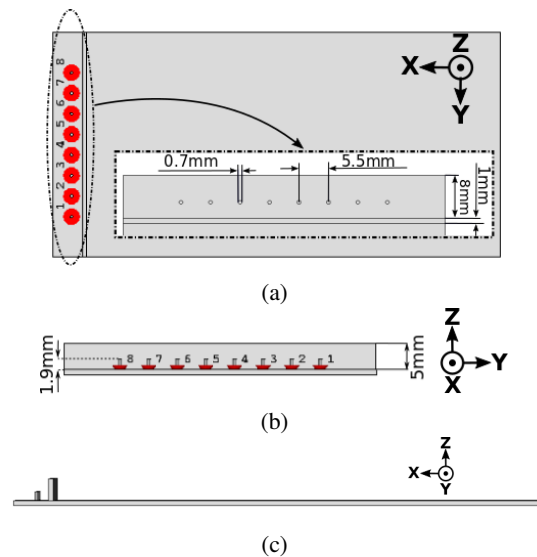

Fig. 2. Geometry of the proposed 28 GHz monopole array in (a) xy-plane, (b) yz-plane, and (c) xz-plane.

this purpose. The monopole elements have a height of 1.9 mm and distance a between them is 5.5 mm($\lambda/2$).

It has been selected to consider four different scan angles of the array. The chosen scan angles of 28°, 58° , 90° and 128° are illustrated in Fig. 3
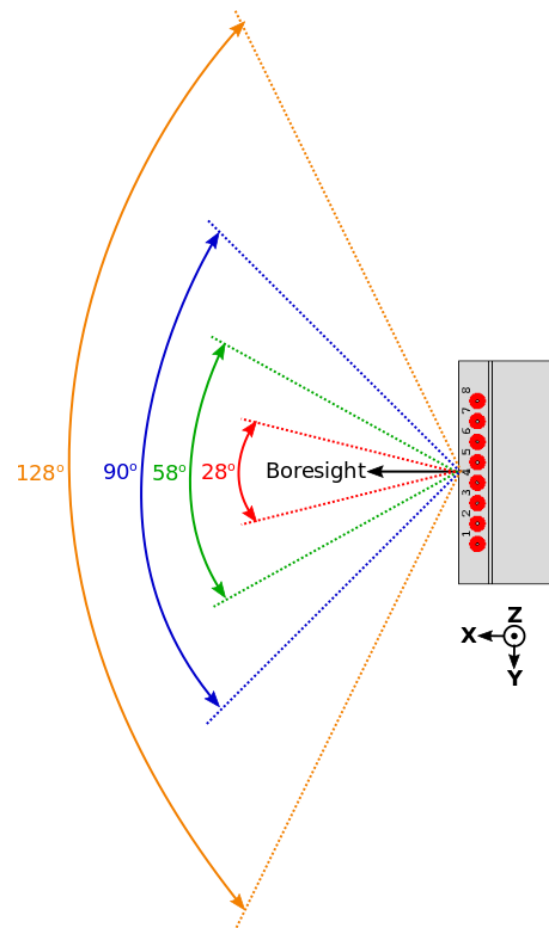

Fig. 3. Illustration of the four array's scan angles used in investigation.

In Fig. 4 the TSPs of the array with different scan angles.

This wide scan angle behavior is expected because each of the antenna elements have a radiation pattern with a wide main beam. Furthermore, the SD pattern of the antenna array is shown in Fig. 4(e). The SD pattern is calculated by switching among 8 available antennas, instead of using the phase shifters to change the beam direction of the phased array. The SD pattern of the proposed antenna array is considerably weaker.
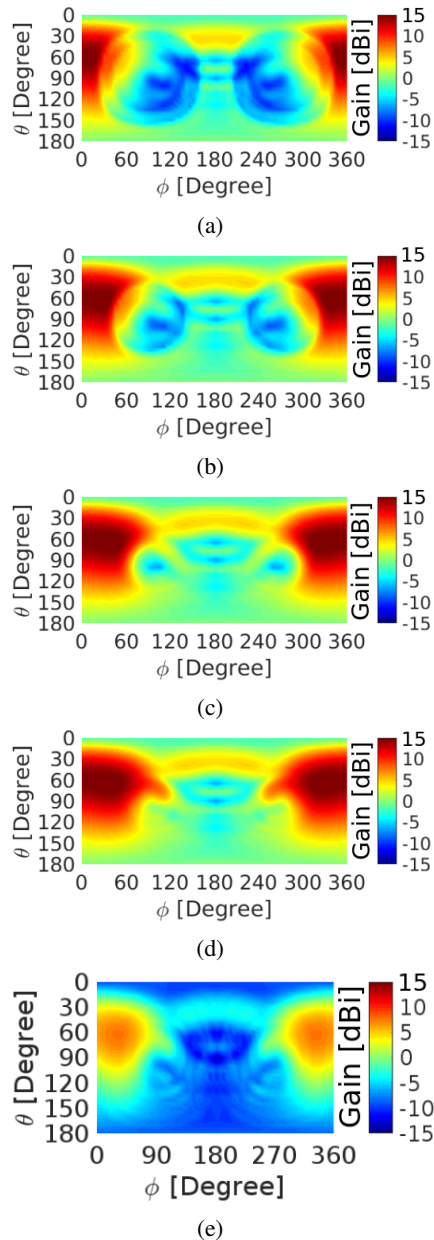

(a)

(b)

(c)

(d)

(e)

Fig. 4. Total scan patterns of the phased antenna array at 28 GHz in free space for (a) 28° scan angle, (b) 58° scan angle, (c) 90° scan angle, (d) 128° scan angle, and (e) SD pattern.

To investigate the spatial performance of the phased antenna array the coverage efficiency metric is used. Coverage efficiency is defined as [6]:

$$\eta_c = \frac{\text{Coverage Solid Angle}}{\text{Maximum Solid Angle}} \quad (1)$$

where maximum solid angle defined as 4π steradians in order to account for the arbitrary angle of arrival and arbitrary

orientation of the mobile device. The coverage efficiency is calculated from the total scan pattern with respect to the chosen set of the gain values. Here it has been chosen to use gain values ranging from -10 to 15 dBi.
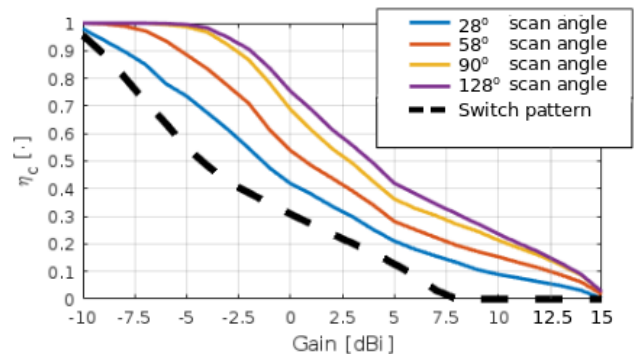

Fig. 5. Coverage efficiency of the proposed phased antenna array in free space.

The coverage efficiency of the proposed antenna array in free space is shown for all four chosen phase shift steps in Fig. 5. The coverage efficiency of SD pattern antenna array is also shown in Fig. 5. The difference in the coverage efficiency between blue, red and yellow curves is around 10 % at 0 dBi gain and becomes smaller as gain increases. The difference between the dashed curve for the SD pattern antenna array and the worst of the phased antenna array curves is 5 % for the gain range from 0 dBi to 7.5 dBi. It can clearly be seen that phased antenna array is much more efficient than the SD pattern array in free space.

III. USER IMPACT

In this section, the performance of the phased array with different scan angles and the SD antenna array will be investigated with the human phantom in data mode. The simulation setup with the phantom is shown in Fig. 6. It is important to notice that it is difficult to make the user sit/stand still for a prolonged period of measurement time. The errors due to user movement will lead to the phase instability in the measurement. The beamforming cannot be performed correctly when the measured radiation patterns have an incorrect phase, however when measuring the SD array the phase errors are not important because only magnitude of the radiation pattern is of interest. Thus, the simulations of the phased array are more reliable than the measurements. At this current moment, no standards for human gestures have been defined for cm/mm-wave 5G mobile terminals. Thus, it has been chosen to use the proposed full-body realistic phantom [12] and simulate it in CST Microwave Studio FDTD solver. The length of the limbs, body circumference and weight of the phantom has been based on the average values for human male, defined in [13] and [14]. The hand gesture of the phantom complies with the CTIA standards for data mode [15]. The dimensions of the phantom can be found in Table I.

The homogeneous full-body male phantom is made of skin tissue with real and imaginary parts of $\varepsilon_r = 16.5 + j16.5$. The parameters of different tissues up to 100 GHz have been measured in [16]. A homogeneous model has been used

because at the 28 GHz the waves will not penetrate deep into human tissue. For instance, the skin depth at 28 GHz can be calculated to 1.158 mm if a resistivity of the human tissue of 245 Ωcm [17] has been used in calculations.
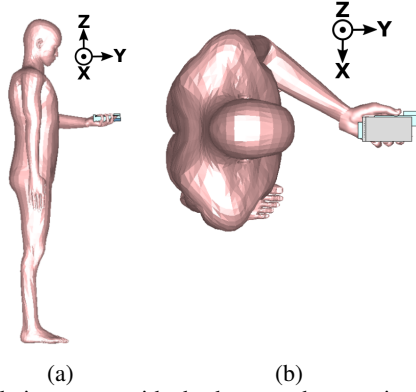

(a)   (b)

Fig. 6. Simulation setup with the human phantom in (a) side view and (b) top view.

Table I. Dimensions of the phantom and the measured user.

Category	Phantom	User
Height	175.6 cm	174 cm
Neck circumference	42.8 cm	43 cm
Upper arm length	25 cm	24 cm
Upper arm circumference	27.8 cm	32 cm
Lower arm length	27 cm	27.7 cm
Wrist circumference	15 cm	16 cm
Chest circumference	108 cm	111 cm
Waist circumference	89 cm	86 cm
Hip circumference	101 cm	97 cm
Upper leg length	40 cm	40 cm
Lower leg length	50 cm	45 cm
Ankle circumference	22 cm	22 cm

A. Phased Antenna Array

The simulated total scan patterns of the phased antenna array with the human phantom are shown in Fig. 7. It can clearly be seen that more space around the user can be covered if larger scan angle of the antenna array is used, but the power in the shadowing area almost remains the same.

The dependency of the scan angle of a phased array on shadowing antenna power ratio (SAPR), shadowing isotropic antenna power ratio (SIAPR), and coverage efficiency is also investigated, which is shown in Fig. 8. The SAPR and SIAPR are defined as [9]:

$$SAPR(\Delta\theta, \Delta\phi) \triangleq \frac{P_{shadow\ in\ the\ window}(\Delta\theta, \Delta\phi)}{P_{total}} \quad (2)$$
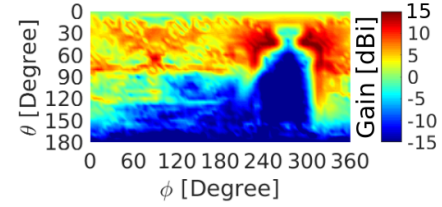
$$SIAPR(\Delta\theta, \Delta\phi) \triangleq \frac{P_{shadow\ in\ the\ window}(\Delta\theta, \Delta\phi)}{P_{isotropic}} \quad (3)$$
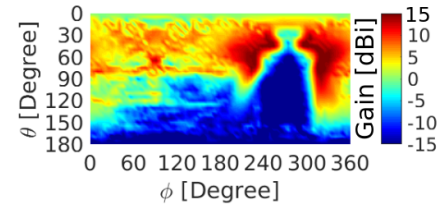
where:
- $\Delta\theta$ is the window size in θ
- $\Delta\phi$ is the window size in ϕ
- $P_{shadow\ in\ the\ window}(\Delta\theta, \Delta\phi)$ is the power in the window of the chosen size.
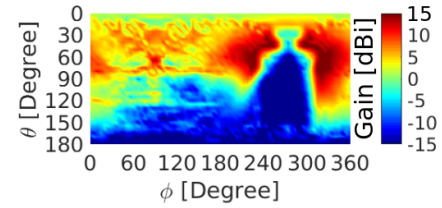- P_{total} is the total radiated power (TRP) of the antenna.
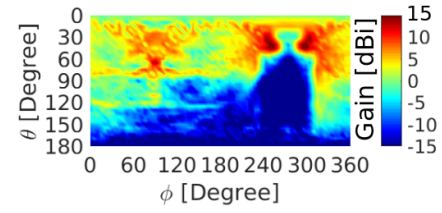
Fig. 7. Simulated at 28 GHz total scan patterns of the phased antenna array with the user with (a) 28° scan angle, (b) 58° scan angle, (c) 90° scan angle, (d) 128° scan angle.

- $P_{isotropic}$ is the total radiated power of the isotropic antenna if transmit power is 0 dB.

The SAPR and SIAPR metrics describe how much the power in the shadowing area is lower than the TRP of the reference antenna. The SAPR parameter depends on the antenna design, because the TRP of the chosen antenna is used. The TRP will vary, depending of the antenna efficiency. However, the SIAPR parameter is not antenna specific because the TRP of the isotropic antenna is used in the equation, which is constant.

In this paper, the $\Delta\theta$ window width is constant and chosen to the maximum of 180° (or 140° because of the measurement system constraints) because the shadowing from the user's body spans along the full range of the elevation plane. Then, SAPR and SIAPR are calculated for the $\Delta\phi$ values from 1 to 90°. In Fig. 8(a) the difference in the SAPR for the phased antenna array performing with different scan angles is very small. It occurred because SAPR metric uses total power as a reference, where total power is not constant. This means that power in the shadow does not change with respect to the total power. However, the SIAPR in Fig. 8(b) have different values for the window sizes larger than $\theta = 30°$. The difference of 2.5 dB can be observed for the window sizes

larger than $\theta = 30°$. Furthermore, there is no difference in the performance of the antenna arrays with 90° and 128° scan angles. The difference in the coverage efficiency is very small for the phased antenna arrays with 58°, 90°, and 128° scan angles due to scattering by the user's body.
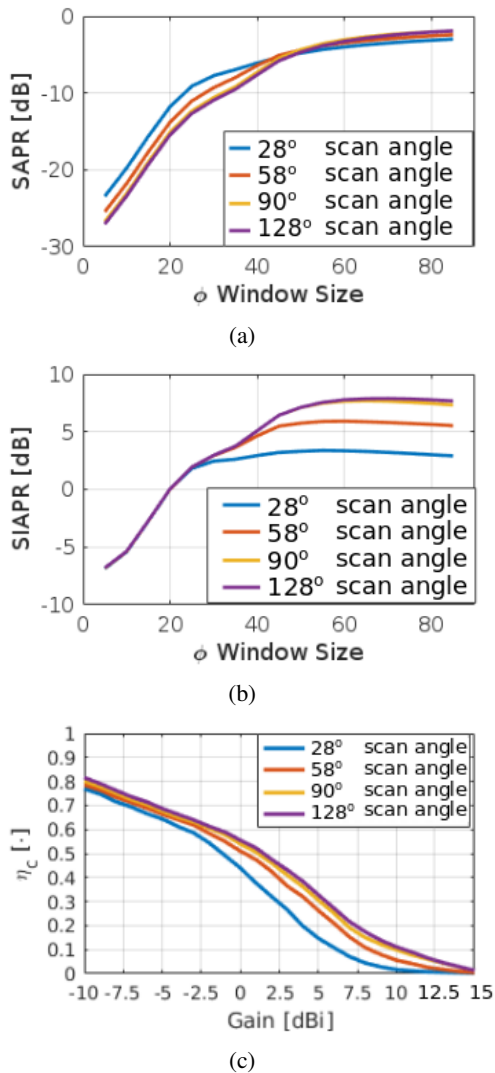

(a)

(b)

(c)

Fig. 8. Plots of (a) SAPR, (b) SIAPR, and (c) coverage efficiency of the phased antenna array with the user at 28 GHz

B. Switch Diversity Antenna Array

In this subsection, the SD antenna array performance is measured and simulated by using the same setup, described in Sec. III-A. The simulations have been done in CST Microwave Studio using the time domain solver. The 876 million mesh cells have been used in the simulation. The smallest mesh cell size is 0.044 mm and the biggest mesh cell size is 0.856 mm. The mesh is denser in the locations where the currents are strong. On the other hand, the measurements have been done in the anechoic chamber with a single dual-polarized probe antenna. The resolution of 14° in the elevation plane and 2° in azimuth plane has been chosen. The coarse resolution in the elevation plane has been chosen in order to reduce the measurement time. Shorter measurement time will ensure that

the person under the test can stand still without significant discomfort. Because of the measurement system limitations, only the elevation angles up to 140° could be measured. The 10 frequency points have been measured for each position of the probe antenna, however only results at 28 GHz have been presented in this paper. However, a real human specimen has been used in the measurement instead of a phantom. The dimensions of the human under test is shown in Table I. Actually, many of the major dimensions of the human and phantom are similar. Furthermore, the simulations and measurements of the SD array are compared to the phased array in this section. The phased array antenna performance has not been measured with the user because the phase is unstable in the proposed measurement setup with available measuring equipment. To verify the simulated results, the prototype of the mobile phased monopole antenna array has been constructed. The geometry of the prototype is shown in Fig.9. No feeding network has been constructed, and instead, each of the monopoles has its own cable of the same length.
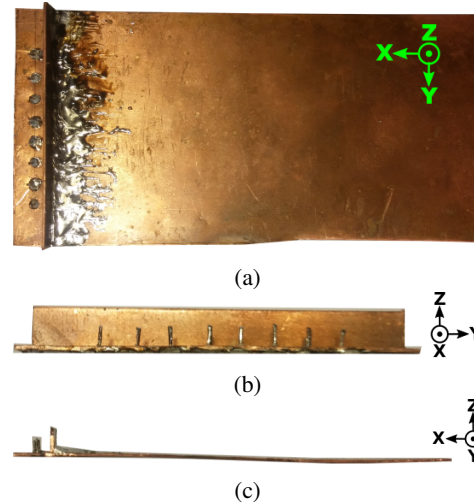

(a)

(b)

(c)

Fig. 9. Geometry of monopole antenna array prototype in (a) xy-plane, (b) yz-view, and (c) xz view.

First, the antenna array prototype has been measured in the free space, as shown in Fig. 10(a), and then it has been measured with the user, as shown in Fig. 10(b). For the free space case the coordinate system is different from the simulations because the prototype has been rotated in order to get easier access to the cables. All of the measurements have been done in the anechoic chamber. The user has similar height as the phantom, but different build. Furthermore, the effects of the clothes have not been included in the simulations.

Then, it has been chosen to compare the radiation patterns of the simulated and measured antennas in the free space. The comparison of the measured and simulated patterns of the center element 4 and the edge element 8 are shown in Fig. 11. The gain of the measured radiation patterns is on average 1 dB higher than the gain of the simulated radiation patterns. The edge element has a slightly different pattern than the center element, which is expected because of the edge effects.

Usually, the measurement will have inaccuracies such as movement of the user under the measurement, different phone
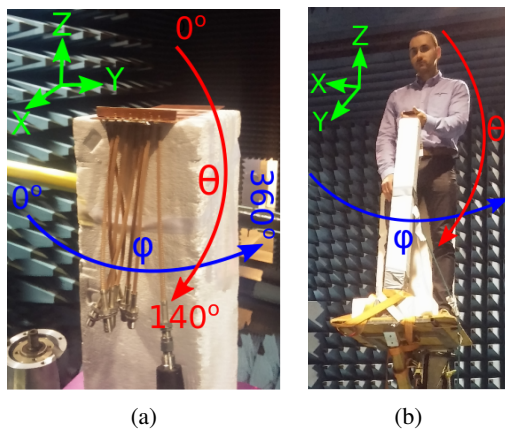
This article has been accepted for publication in a future issue of this journal, but has not been fully edited. Content may change prior to final publication. Citation information: DOI 10.1109/ACCESS.2017.2779792, IEEE Access

6

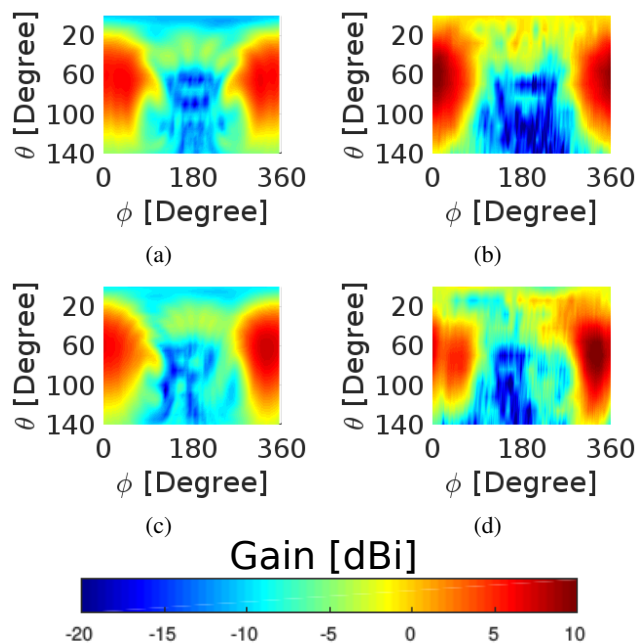Fig. 10. Measurement setup in (a) free space and (b) with the user.

Gain [dBi]

Fig. 11. Radiation patterns of (a) simulated element 4, (b) measured element 4, (c) simulated element 8, and (d) measured element 8 at 28 GHz.
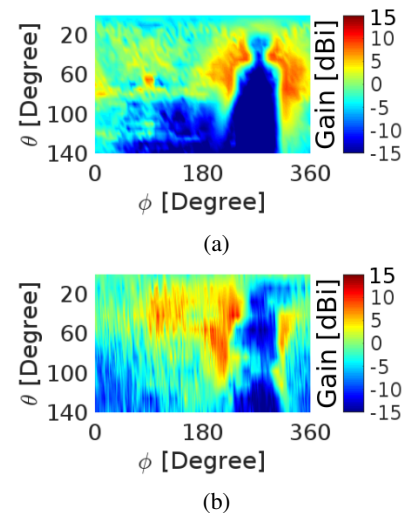

Fig. 12. Total SD pattern of (a) simulated antenna array and (b) measured antenna array.

the simulation results follow the measurements very well. It has been chosen to compare the switch diversity array to the phased array low scan angle of 28° because the highest SAPR and similar SIAPR for all of the scan angles of the phased antenna array can be observed for the small window sizes (Fig. 8(a) and Fig. 8(a)). The curve for the low phased array scan angle of 28° has also been added to the figures of coverage efficiency, SAPR, and SIAPR in Fig. 13. The difference between the coverage efficiency curves for the switchable pattern array and phased array with 28° scan angle is on average 5 to 10 % in Fig. 13(a). The difference in coverage efficiency decrease for the high gains ≥ 7.5 dBi. In Fig. 13(b) the SAPR difference between phased array with 28° scan angle and switchable pattern array is around 5 dB for the window sizes less than 30°. The SIAPR of the phased array with the scan angle of 28° is 5 dB higher than SIAPR of SD array for window sizes less than 40°.

IV. CONCLUSION

In this paper, the switch diversity antenna array has been compared to the phased mobile antenna array with different scan angles by simulating and measuring in free space and with a standing user in data mode. The investigation has been done at 28 GHz. For the linear endfire phased arrays on the short edge of the ground plane it can be concluded that in order to achieve the highest coverage efficiency and lowest user shadowing it is always more beneficial to use phased array than the switched pattern antenna array. However, this is concluded based on the assumption that the combined losses of the phase shifters and feeding network is less than 5 dB.

The increase in coverage efficiency of up to 30 % at the gain of 7.5 dBi in the free space can be achieved if the phased array with a scan angle bigger than 90° in comparison to the switch diversity array. The increase in coverage efficiency of up to 20 % at the gain of 7.5 dBi is expected when the antenna array is used by the user in data mode. However, scan angles bigger than 90° does not increase the coverage performance dramatically. The SAPR and SIAPR for the window sizes less than 30° are very similar for all of the chosen scan angles.

grip, random effect of clothing. Furthermore, the phase is very challenging to control accurately at 28 GHz when measurements are done with the user. Even a small user movement will result in the phase error in the order of hundreds of degrees. Thus, the beamforming cannot be performed if the phase stability requirement is not satisfied. Because of the phase stability issue, only the measured SD patterns are considered in this section. The total SD patterns of the simulated and measured with the user antenna arrays are shown in Fig. 12. The measured total SD pattern is more noisy and less power is present on the right side of the user ($\phi = 330°$), because of the user's grip difference. However, the user's shape is still visible at $\phi = 270°$.

Finally, to investigate the performance difference of the simulated and measured antenna arrays with the user, it has been chosen to calculate coverage efficiency (Fig 13(a)), SAPR (Fig. 13(b)), and SIAPR (Fig. 13(c)). In all of the figures,
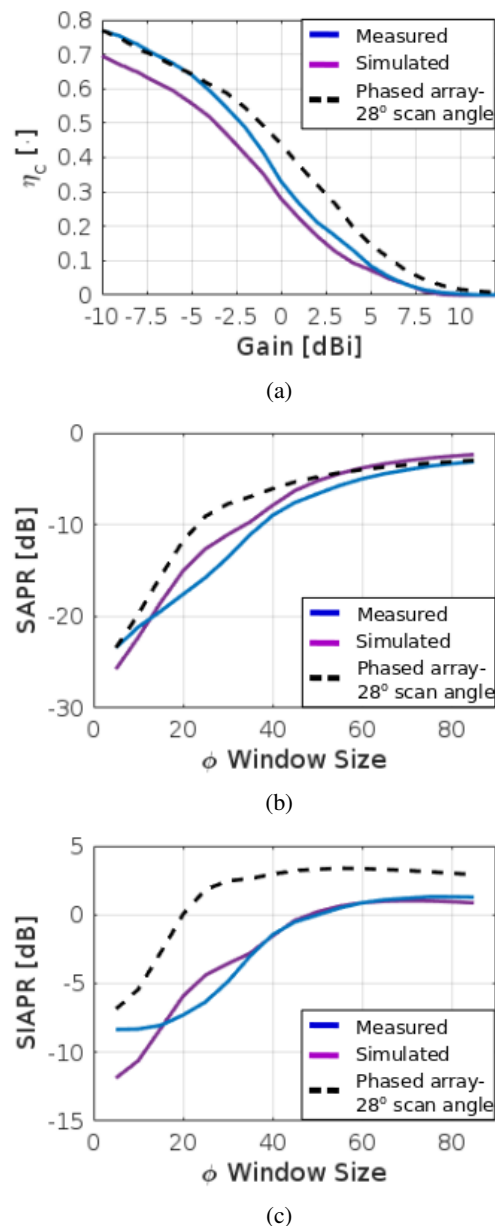
Fig. 13. Plots of (a) total SD pattern of the array, (b) SAPR, and (c) SIAPR of the SD antenna array with the user.

In this case, most of the energy radiating from the antenna is blocked and only a small portion of the energy is scattered around the body.

The SAPR is on average 5 dB and SIAPR is 5 to 7 dB lower for the switch diversity antenna array than the phased antenna array. In practice, if the losses of the phase shifters and feeding network is higher than 5 dB the switch diversity antenna array can be used in the studied scenario, which will also decrease the complexity of a system.

Finally, it can be noticed that the results may change with both antenna array location, radiation pattern direction (broadside or endfire) and body position (position of the mobile terminal with respect to the user's body). Nonetheless, the orientation of the mobile can still be very random. Such factors as hand grip (two hands - horizontal orientation , one hand horizontal orientation, one hand vertical orientation, etc.), different angle of the arm, and distance from the antenna to

the body will influence the size of the shadowing region and performance of the phased antenna array system. However the conclusion of the paper is still very useful and meaningful because user's body will always scatter the field and contribute to the total radiation of antenna. Thus, large scan angle of the phased array is not always beneficial in order to obtain the good coverage efficiency. Furthermore, because the phased array and and SD array using the same array configuration and elements, so even if the conditions (antenna pattern, type, body location, etc.) may change the relative relations in the shadowed region between SD and phased array will be similar.

REFERENCES

[1] T. S. Rappaport, S. Sun, R. Mayzus, H. Zhao, Y. Azar, K. Wang, G. N. Wong, J. K. Schulz, M. Samimi, and F. Gutierrez, "Millimeter wave mobile communications for 5G cellular: It will work!," *IEEE Access*, vol. 1, pp. 335–349, 2013.

[2] W. Roh, J. Y. Seol, J. Park, B. Lee, J. Lee, Y. Kim, J. Cho, K. Cheun, and F. Aryanfar, "Millimeter-wave beamforming as an enabling technology for 5G cellular communications: theoretical feasibility and prototype results," *IEEE Commun. Mag.*, vol. 52, pp. 106–113, feb 2014.

[3] N. Ojaroudiparchin, M. Shen, S. Zhang, and G. F. Pedersen, "A switchable 3-d-coverage-phased array antenna package for 5g mobile terminals," *IEEE Antennas and Wireless Propag. Lett.*, vol. 15, pp. 1747–1750, 2016.

[4] S. Zhang, X. Chen, I. Syrytsin, and G. F. Pedersen, "A planar switchable 3D-coverage phased array antenna and its user effects for 28 GHz mobile terminal applications," *IEEE Trans. Antennas Propag.*, vol. 65, pp. 6413 – 6421, 2017.

[5] M. U. Rehman, X. Chen, C. G. Parini, and Z. Ying, "Evaluation of a statistical model for the characterization of multipath affecting mobile terminal GPS antennas in sub-urban areas," *IEEE Trans. Antennas Propag.*, vol. 60, pp. 1084–1094, Feb 2012.

[6] J. Helander, K. Zhao, Z. Ying, and D. Sjöberg, "Performance analysis of millimeter-wave phased array antennas in cellular handsets," *IEEE Antennas Wireless Propag. Lett*, vol. 15, pp. 504–507, 2016.

[7] K. Zhao, J. Helander, D. Sjoberg, S. He, T. Bolin, and Z. Ying, "User body effect on phased array in user equipment for 5G mm wave communication system," *IEEE Antennas Wireless Propag. Lett*, vol. PP, no. 99, p. 1, 2016.

[8] J. B. Andersen, J. O. Nielsen, and G. F. Pedersen, "Absorption related to hand-held devices in data mode," *IEEE Transactions on Electromagnetic Compatibility*, vol. 58, pp. 47–53, Feb 2016.

[9] I. Syrytsin, S. Zhang, G. F. Pedersen, K. Zhao, T. Bolin, and Z. Ying, "Statistical investigation of the user effects on mobile terminal antennas for 5G applications," *IEEE Trans. Antennas Propag.*, vol. 65, pp. 6596 – 6605, 2017.

[10] S. Obayashi and J. Zander, "A body-shadowing model for indoor radio communication environments," *IEEE Trans. Antennas Propag.*, vol. 46, pp. 920–927, Jun 1998.

[11] N. Tran, T. Imai, and Y. Okumura, "Study on characteristics of human body shadowing in high frequency bands: Radio wave propagation technology for future radio access and mobile optical networks," *2014 IEEE 80th Vehicular Technology Conference (VTC2014-Fall)*, pp. 1–5, 2014.

[12] I. Syrytsin, S. Zhang, G. F. Pedersen, and Z. Ying, "User effects on circular polarization of 5G mobile terminal antennas," *IEEE Trans. Antennas Propag.*, 2017 (Submitted).

[13] J. Panero and M. Zelnik, *Human dimension and interior space: A source book of design reference standards*. Watson-Guptill, 1979.

[14] Health Examination Survey, The National Health and Nutrition Examination Surveys, and The Hispanic Health and Nutrition Examination Survey, *Anthropometric reference data for children and adults: United States, 2007–2010*. U.S. Government Printing Office, 2012.

[15] C. Telecommunications and I. A. (CTIA), "Test plan for wireless device over-the-air performance," *Revision Number 3.6.1*, November 2016.

[16] C. Gabriel, S. Gabriel, and E. Corthout, "The dielectric properties of biological tissues: I. literature survey," *Phys. Med. Biol.*, vol. 41, p. 2231–2249, 1996.

[17] H. C. Burger and R. van Dongen, "Specific resistance of body tissues," *Phys. Med. Biol.*, vol. 5, no. 4, pp. 431–447, 1961.